Journal of Engineering Mathematics, Vol. 9, No. 1, January 1975
Noordhoff International Publishing–Leyden
Printed in The Netherlands

A new calculation of the wake of a flat plate

A. E. P. VELDMAN

Department of Mathematics, University of Groningen, Groningen, The Netherlands.

(Received August 9, 1974)

SUMMARY

A new method is presented for the calculation of the wake of a finite flat plate. The method is based upon the recent investigations of the boundary layer near the trailing edge, which led to the triple-deck structure. This multi-layered structure has now been extended to the "classical" wake, which in fact is the continuation of the lowest two layers of the triple-deck. With this new numerical formulation an accuracy of $10^{-3}\%$ can easily be achieved.

1. Introduction

From momentum observations it is known that, in boundary layer theory, the drag of a body equals the momentum thickness far behind the body (Schlichting [1]). For a finite flat plate of length L, placed in a uniform stream parallel to the plate with velocity U, density ρ and viscosity ν, the drag on one side of the plate is given by

$$D = 2a\rho U^2 L \,\mathrm{Re}^{-\frac{1}{2}} + \ldots , \tag{1}$$

where a is the Blasius constant $a = 0.332057$ and $\mathrm{Re} = UL/\nu$ is the Reynolds number. In fact for a flat plate the momentum thickness must equal D for *all* $x \geqq 0$, $x = 0$ being the trailing edge.

First attempts to calculate the flow field in the wake were made by Tollmien [2] and Goldstein [3, 4]. They set up asymptotic expansions valid for either $x \to 0$ [3] or $x \to \infty$ [2]. Goldstein [4] tried to patch these two expansions. However, a verification of the equality of the drag and the momentum thickness could not be made, because the expansion for $x \to \infty$ contained an arbitrary constant which had to be evaluated by imposing this equality.

The only possibility for verification is to solve the boundary layer equations for all x, starting with the correct initial profile. Goldstein's expansion near $x = 0$, however, possesses a singularity in the velocity which makes the boundary layer equation no longer valid near $x = 0$. Recently the correct structure of the flow field near the trailing edge has been determined by Stewartson [5] and Messiter [6]. They suggested a triple-deck structure in a region where $x = O(\mathrm{Re}^{-\frac{3}{8}})$. This triple-deck consists of three layers: (i) a viscous sublayer where $y = O(\mathrm{Re}^{-\frac{5}{8}})$ and the boundary layer equation with pressure gradient must be used; (ii) an inviscid main deck where $y = O(\mathrm{Re}^{-\frac{1}{2}})$ and the main term in the streamfunction is the Blasius function; (iii) a potential upper deck where $y = O(\mathrm{Re}^{-\frac{3}{8}})$, which smoothes out the disturbances of the boundary layer. The equations governing the flow in the triple-deck have been solved by Veldman and van de Vooren [7], Burggraf and Jobe [8] and Melnik [9].

From the triple-deck investigations we can obtain a good insight into the structure of the initial profile of the wake boundary layer. At first sight the initial profile is given by the Blasius solution. Calculations of the wake using this starting profile have already been made by Charwat and Schneider [10] and by Vasantha and Narasimha [11]. They claim to have calculated a momentum thickness which is constant in x-direction within 1% and 0.1% respectively. A closer examination learns that a better starting profile is obtained when we also take into account the existence of the sublayer in the triple-deck. Therefore we split the near wake into two regions. One which matches the inviscid main deck and one which matches the sublayer. These two regions are the same as Goldstein's outer and inner region [3].

In the sublayer of the triple-deck for $x \geqq 0$ an analogous structure exists. In the triple-deck calculations of Veldman and van de Vooren [7] the sublayer was divided into an upper and a lower part, analogous to Goldstein's outer and inner region. It was found that this splitting is an accurate way in handling the flow singularities near $x=0$. Therefore we will use in this paper the method of Veldman and van de Vooren to calculate the wake. This idea of splitting the wake was also proposed by Smith [12]. It appears that the accuracy of the calculations can easily be improved down to $10^{-3}\%$.

2. Numerical method

Let (x, y) be a Cartesian coordinate system with origin at the trailing edge of the plate, non-dimensionalized by L. The velocity will be nondimensionalized by U and the streamfunction ψ by UL. In the boundary layer we introduce a stretching transformation $y=\mathrm{Re}^{-\frac{1}{2}}\tilde{y}$ and $\psi=\mathrm{Re}^{-\frac{1}{2}}\tilde{\psi}$. Then the boundary layer equation in the wake is written as

$$\tilde{\psi}_{\tilde{y}}u_x-\tilde{\psi}_x u_{\tilde{y}}=u_{\tilde{y}\tilde{y}}\,,\quad \tilde{\psi}_{\tilde{y}}=u \tag{2a, b}$$

with boundary conditions

$$\tilde{y}=0:\ \tilde{\psi}=u_{\tilde{y}}=0\ ;\ \tilde{y}\to\infty:\ u\to 1 \text{ exponentially}\,. \tag{3}$$

For small x, the solution is given by the Goldstein inner solution which matches the sublayer of the triple-deck

$$\tilde{\psi}\sim x^{\frac{2}{3}}f_0(\eta) \tag{4}$$

where $\eta=\tilde{y}x^{-\frac{1}{3}}$ and f_0 satisfies $f_0'''+\frac{2}{3}f_0f_0''-\frac{1}{3}f_0'^2=0$ with boundary conditions $f_0(0)=f_0''(0)=0$, $f_0''(\infty)=a$, and by the Goldstein outer solution which matches the main deck of the triple-deck

$$\tilde{\psi}\sim F_0(\tilde{y})+x^{\frac{1}{3}}A_1F_0'(\tilde{y}) \tag{5}$$

where F_0 is the Blasius function satisfying $F_0'''+\frac{1}{2}F_0F_0''=0$, $F_0(0)=F_0'(0)=0$, $F_0'(\infty)=1$ and $A_1=1.288129$.

For large x the solution is given by

$$\tilde{\psi}\sim x^{\frac{1}{2}}\zeta-A\pi^{\frac{1}{2}}\operatorname{erf}(\tfrac{1}{2}\zeta) \tag{6}$$

where $\zeta=yx^{-\frac{1}{2}}$ and from momentum considerations we should have $A=2a/\pi^{\frac{1}{2}}$. See for instance Schlichting [1] or Berger [13].

Due to the different behaviour of the far and the near wake we have split the wake into two parts: $x\leqq 1$ and $x>1$. In the part $x\leqq 1$ we use variables especially suited for the near wake structure; in the part $x>1$ other variables, adapted to the far wake are used. In $\tilde{y}$-direction the wake has been cut off at some finite value of $\tilde{y}$. This is possible because the horizontal velocity u approaches its free stream value exponentially.

The region $x\leqq 1$: The wake is divided into two parts. A lower region where the η-coordinate is finite and an upper region where the $\tilde{y}$-coordinate should be used. In the lower region we set

$$\tilde{\psi}=x^{\frac{2}{3}}\bar{\psi}\,,\quad u=x^{\frac{1}{3}}\bar{u}\,. \tag{7}$$

Moreover a transformation in the η-coordinate is used to obtain a better spreading of the meshpoints in η-direction.

$$\eta=t+(\alpha-1)t^3\,,\quad t\in[0,1]\,. \tag{8}$$

Thus the η-region is restricted to $\eta\in[0,\alpha]$. The value of α must be large enough to allow f_0 reach its asymptotic behaviour for large η. The same transformation was used in [7].

In the upper region we take

$$\tilde{\psi}=\tilde{y}+\hat{\psi}\,,\quad u=1+\hat{u}\,. \tag{9}$$

In this way $\hat{\psi}$ is bounded and $\hat{u}$ vanishes if $\tilde{y}\to\infty$.

The appropriate variable in x-direction is $x^{\frac{1}{3}}$. But an additional transformation to obtain even more points near $x=0$ appears preferable. Therefore we take

$$x^{\frac{1}{3}}=\tfrac{1}{2}\sigma+\tfrac{1}{2}\sigma^2\,,\quad \sigma\in[0,1]\,. \tag{10}$$

The grid points in the upper and lower region should be smoothly connected. Therefore we have to make the following transformation in $\tilde{y}$-direction

$$\tilde{y}=\tfrac{1}{2}\alpha(\mu+\mu^2)\,,\quad \mu\in[0,1]\,. \tag{11}$$

The values of $\tilde{y}$ are restricted to $[0, \alpha]$, which implies that α must be large enough to cover the whole boundary layer. A value $\alpha=10$ appears to be large enough.

The region $x>1$: In the far wake, equation (6) suggests to set

$$\tilde{\psi}=x^{\frac{1}{2}}\zeta+\psi^*\,,\quad u=1+x^{-\frac{1}{2}}u^*\,. \tag{12}$$

This region is only connected with the lower region $x\leqq 1$. In ζ-direction we can therefore also make use of transformation (8). In x-direction the simplest possible transformation

$$x^{-\frac{1}{2}}=1-s\,,\quad s\in[0,1] \tag{13}$$

appears to be satisfactory.

A rough sketch (not to scale) of the total grid structure is displayed in Fig. 1.

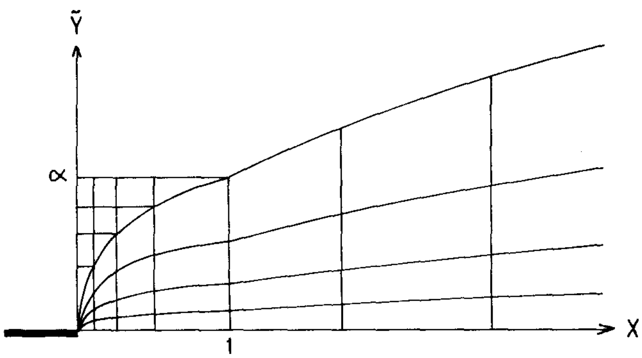

Figure 1. The grid structure.

The equations have been solved by a finite difference method. A grid was used, equidistant spaced in the σ, μ, t and s variables. When in the σ-interval $[0, 1]$ N points were chosen, the μ- and t-intervals were covered with $4N$ points each and the s-interval with $\frac{1}{2}N$ points. Line iteration has been used along lines $x=$constant, starting at $x=0$. As initial profile we use the Blasius and Goldstein functions, leading to $\bar{\psi}(0,\eta)=f_0(\eta)$ and $\hat{\psi}(0,\tilde{y})=F_0(\tilde{y})-\tilde{y}$.

Equation (2) was transformed by the transformations (7) through (13). The transformed equation (2a) was used as an equation for the transforms of u. It was discretized with a usual Crank–Nicholson method, using points at lines x and $x-\Delta x$. At the boundary between the upper and lower region in $x\leqq 1$ we use the upper formulation. Thus a tridiagonal system of equations is obtained, in which the only exception is made by the boundary condition $u_{\tilde{y}}=0$ at $\tilde{y}=0$. This equation was discretized like $3u(x,0)-4u(x,k)+u(x,2k)=0$. Actually the coordinates (σ, t) or (s, t) were used instead of $(x, \tilde{y})$. The terms $\tilde{\psi}_{\tilde{y}}$ and $\tilde{\psi}_x$ in equation (2) were regarded as coefficients in this u-equation and were calculated from previously found values of $\tilde{\psi}$. In the first iteration-step at a line $x=x_0$, the values of $\tilde{\psi}$ were taken equal to those at $x=x_0-\Delta x$. In the following steps they were calculated by an integration of Eqn. (2b) using the newest values for u.

The iterations at a line stopped when the new values of $\bar{u}$, $\hat{u}$ or u^* did not change more than 10^{-7} in one iteration step. For most of the lines 5–9 iterations were needed. Only very close to $x=0$ a little more were required.

3. Results and conclusions

Calculations have been performed with four different grids: $N=20$, 40, 80 and 160. The computation time on a CDC 6600 for these grids is 9 sec., $\frac{1}{2}$ min., 2 min. and 7 min. respectively.

As a demonstration of the accuracy reached with this new method we present in Table 1 the values of the momentum thickness $\delta_2=\int_0^\infty u(1-u)d\tilde{y}$ and of $u^*(\infty, 0)$ at $s=1$ $(x=\infty)$,

TABLE 1

Values for momentum thickness and velocity defect at $x=\infty$

	$\delta_2(\infty)$	$u^*(\infty, 0)$
$N=20$	0.659594	−0.372904
$N=40$	0.662952	−0.374219
$N=80$	0.663815	−0.374564
$N=160$	0.664036	−0.374654
Extrapolated 20– 40	0.664071	−0.374657
40– 80	0.664103	−0.374679
80–160	0.664110	−0.374684
Exact	0.664115	−0.374687

TABLE 2

Values for centerline velocity $u(x, 0)$, displacement thickness $\delta_1(x)$ and its derivative $d\delta_1(x)/dx$, obtained with a Richardson extrapolation.

x	$u(x, 0)$	$\delta_1(x)$	$d\delta_1(x)/dx$
0	0	1.720788	$-\infty$
1.80879×10^{-5}	0.020277	1.686989	-6.2227×10^{2}
1.66375×10^{-4}	0.042484	1.650081	-1.4111×10^{2}
6.41619×10^{-4}	0.066615	1.610219	-5.6900×10
1.72800×10^{-3}	0.092658	1.567624	-2.9016×10
3.81470×10^{-3}	0.120587	1.522582	-1.6804×10
7.41488×10^{-3}	0.150364	1.475450	-1.0528×10
1.31861×10^{-2}	0.181921	1.426656	-6.9508
2.19520×10^{-2}	0.215162	1.376698	-4.7583
3.47257×10^{-2}	0.249952	1.326128	-3.3413
5.27344×10^{-2}	0.286106	1.275544	-2.3885
7.74450×10^{-2}	0.323385	1.225570	-1.7285
1.10592×10^{-1}	0.361495	1.176821	-1.2610
1.54206×10^{-1}	0.400087	1.129882	-9.2441×10^{-1}
2.10645×10^{-1}	0.438767	1.085270	-6.7946×10^{-1}
2.82623×10^{-1}	0.477115	1.043409	-4.9997×10^{-1}
3.73248×10^{-1}	0.514705	1.004608	-3.6798×10^{-1}
4.86051×10^{-1}	0.551132	0.969053	-2.7083×10^{-1}
6.25026×10^{-1}	0.586037	0.936804	-1.9935×10^{-1}
7.94666×10^{-1}	0.619131	0.907813	-1.4684×10^{-1}
1.00000	0.650202	0.881941	-1.0813×10^{-1}
1.23457	0.677866	0.859961	-8.1196×10^{-2}
1.56250	0.707556	0.837432	-5.8257×10^{-2}
2.04082	0.739298	0.814506	-3.9552×10^{-2}
2.77778	0.773046	0.791382	-2.4996×10^{-2}
4.00000	0.808648	0.768307	-1.4348×10^{-2}
6.25000	0.845826	0.745570	-7.1888×10^{-3}
1.11111×10	0.884157	0.723483	-2.9233×10^{-3}
2.50000×10	0.923078	0.702365	-8.2144×10^{-4}
1.00000×10^{2}	0.961925	0.682499	-9.5786×10^{-5}
∞	1	0.664110	0

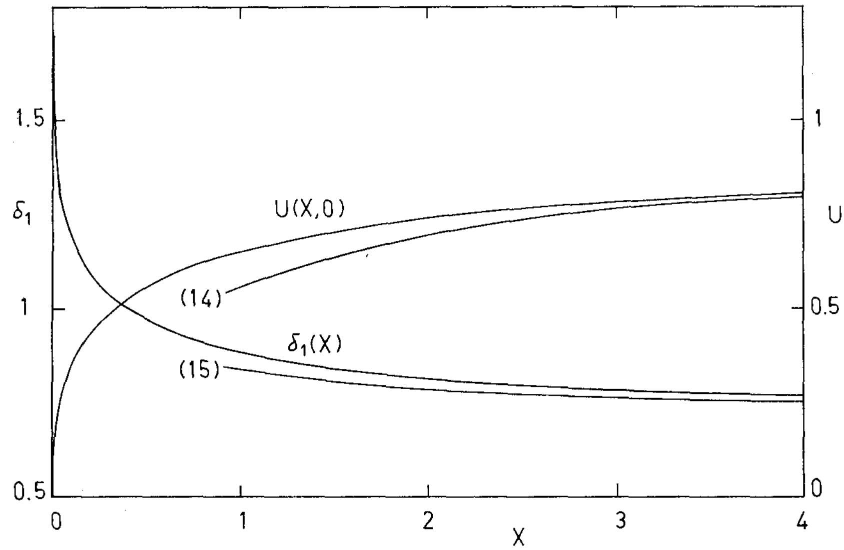

Figure 2. Centerline velocity and displacement thickness in the wake of a flat plate.

TABLE 3

Values for $u(x, 0)$, $\delta_1(x)$ and $d\delta_1/dx$ before extrapolation.

x	$u(x, 0)$		$\delta_1(x)$		$d\delta_1/dx$	
	$N=80$	$N=160$	$N=80$	$N=160$	$N=80$	$N=160$
0.0074	0.150367	0.150364	1.475466	1.475454	-1.0523×10	-1.0527×10
0.1106	0.361472	0.361489	1.176801	1.176816	-1.2621	-1.2612
0.6250	0.586015	·0.586032	0.936496	0.936727	-1.9959×10^{-1}	-1.9941×10^{-1}
2.7778	0.773078	0.773054	0.791062	0.791302	-2.4989×10^{-2}	-2.4994×10^{-2}

which were obtained with the four grids. Also values obtained from a Richardson extrapolation based on h^2 are given.

The exact value for δ_2 is $\delta_2=2a$ and from Eqn. (6) we derive that $u^*(\infty, 0)=-2a/\pi^{\frac{1}{2}}$. Note that the calculations for $N=20$ already find the correct δ_2 within 0.7%. The finest grids even yield after extrapolation an error in δ_2 less than 10^{-3}%. For finite values of x the difference between the calculated δ_2 and its exact value is smaller than at $x=\infty$.

Results for the centerline velocity $u(x, 0)$ and the displacement thickness $\delta_1(x)=\int_0^\infty (1-u)d\tilde{y}$ are given in Table 2 and in Fig. 2. Also shown in Fig. 2 are the far wake asymptotic expansions of these quantities given by

$$u(x, 0)\sim 1-Ax^{-\frac{1}{2}}-\tfrac{1}{2}A^2x^{-1} \text{ and} \tag{14}$$

$$\delta_1(x)\sim A\pi^{\frac{1}{2}}+A^2(\pi/2x)^{\frac{1}{2}}\,. \tag{15}$$

These expansions can be derived from results given by Berger [13].

The second order potential flow outside the wake can be obtained when the vertical velocity at the outer edge of the wake, $\mathrm{Re}^{-\frac{1}{2}}d\delta_1/dx$, is known. Therefore we present in Table 2 also values for $d\delta_1/dx$. All values in Table 2 have been obtained with a Richardson extrapolation from the finest two grids. In order to give an idea of the accuracy of Table 2 we present, for a few values of x, the tabulated quantities before extrapolation in Table 3.

Fig. 3 shows some velocity profiles in the wake, which give an idea of the broadening of the wake for increasing values of x.

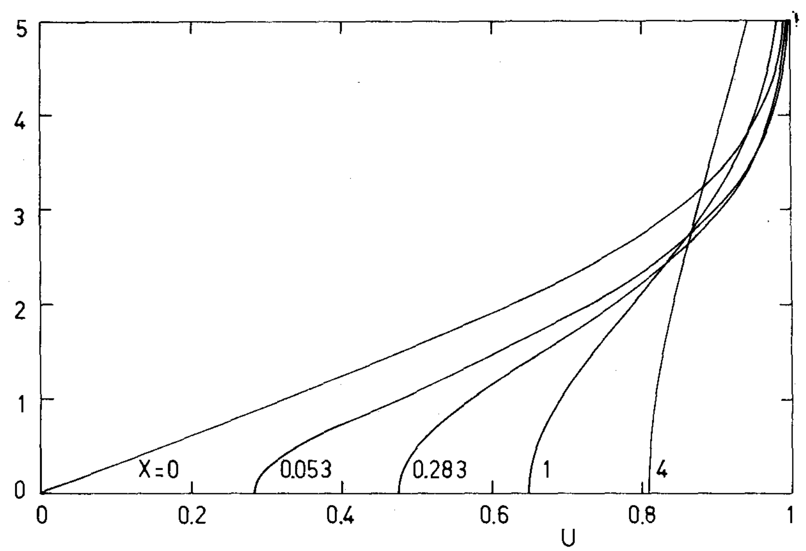

Figure 3. Velocity profiles in the wake of a flat plate.

For interested readers a listing of the computer program, written in Algol 60, is available.

As conclusion we can say that the good understanding of the boundary layer structure near the trailing edge has led to an accurate formulation for the calculation of the wake flow field. It is believed that the basic idea of the method can be used in all problems where triple-decks or other multi-layered structures are present.

REFERENCES

[1] H. Schlichting, *Grenzschichttheorie*, Braun, Karlsruhe (1958).
[2] W. Tollmien, *Grenzschichten, Handb. d. Exper.-Physik IV*, Teil I, 267 (1931).
[3] S. Goldstein, Concerning some solutions of the boundary layer equations in hydrodynamics, *Proc. Cambr. Phil. Soc.* 26 (1930) 1–30.
[4] S. Goldstein, On the two-dimensional steady flow of a viscous fluid behind a solid body, I, *Proc. Roy. Soc.*, A 142, (1933) 545–555.
[5] K. Stewartson, On the flow near the trailing edge of a flat plate, *Mathematika* 16 (1969) 106–121.
[6] A. F. Messiter, Boundary layer flow near the trailing edge of a flat plate, *Siam J. Appl. Math.*, 18 (1970) 241–257.
[7] A. E. P. Veldman and A. I. van de Vooren, Drag of a finite flat plate, *Proc. Fourth International Conference on Numerical Methods in Fluid Dynamics*, Boulder (1974).
[8] O. R. Burggraf and C. E. Jobe, The numerical solution of the asymptotic equations of trailing edge flow, *Proc. Roy. Soc. A*, 340 (1974) 91–111.
[9] R. E. Melnik, Private communication.
[10] A. F. Charwat and L. Schneider, Effect of the boundary layer profile at separation on the evolution of the wake, *AIAAJ*, 5 (1967) 1885–1887.
[11] S. Vasantha and R. Narasimha, A nonlinear theory of wake development, *J. Eng. Math.*, 4 (1970) 51–64.
[12] F. T. Smith, Boundary layer flow near a discontinuity in wall conditions, *J. Inst. Maths. Applics.*, 13 (1974) 127–145.
[13] S. A. Berger, *Laminar wakes*, Elsevier, New York (1971).